


## Article

# A Tribological Study of ta-C, ta-C:N, and ta-C:B Coatings on Plastic Substrates under Dry Sliding Conditions

Paul Neubauer<sup>1</sup>, Frank Kaulfuss<sup>2,\*</sup>  and Volker Weihnacht<sup>2</sup><sup>1</sup> Institut für Fertigungstechnik, Technische Universität Dresden, 01069 Dresden, Germany<sup>2</sup> Fraunhofer Institute for Material and Beam Technology (IWS), Winterbergstr. 20, 01277 Dresden, Germany; volker.weihnacht@iws.fraunhofer.de

\* Correspondence: frank.kaulfuss@iws.fraunhofer.de

**Abstract:** In this study, we analyze the extent to which thin hard coatings can serve as tribological protective layers for the selected plastic substrate materials PA12 (polyamide 12) und PEEK (polyetheretherketone), with and without fiber reinforcement. The approximately 1  $\mu\text{m}$  thick coating variants ta-C, ta-C:N, and ta-C:B, which were applied using the laser arc process, are investigated. In oscillating sliding wear tests against a steel ball in an air atmosphere without lubricant, the wear of the coating and counter body is compared to analogous coating variants applied in parallel to AISI 52100 steel. The ta-C-based coatings show good adhesion strength and basic suitability as wear protection layers on the plastic substrates in the tribological tests. However, there are variations depending on the coating type and substrate material. The use of a Cr interlayer and its thickness also plays an important role. It is demonstrated that by coating under conditions where the uncoated plastic substrate would normally fail, a similarly good performance as with analogously coated steel substrates can be achieved by ta-C:N.

**Keywords:** ta-C; coating; plastic; wear; PA12; PEEK; friction; sliding; tribotest; doped ta-C



**Citation:** Neubauer, P.; Kaulfuss, F.; Weihnacht, V. A Tribological Study of ta-C, ta-C:N, and ta-C:B Coatings on Plastic Substrates under Dry Sliding Conditions. *Lubricants* **2024**, *12*, 331. <https://doi.org/10.3390/lubricants12100331>

Received: 14 August 2024

Revised: 12 September 2024

Accepted: 23 September 2024

Published: 27 September 2024



**Copyright:** © 2024 by the authors. Licensee MDPI, Basel, Switzerland. This article is an open access article distributed under the terms and conditions of the Creative Commons Attribution (CC BY) license (<https://creativecommons.org/licenses/by/4.0/>).

## 1. Introduction

Thin hard coatings, primarily composed of nitride hard materials (e.g., TiN and CrN) or diamond-like carbon (DLC, e.g., a-C:H and ta-C), have been proven to be effective for decades as tribological protective layers on sliding components made of steel. Due to their high hardness, they enhance the surfaces' resistance to micro-abrasive wear and, in some cases, significantly reduce friction. Such coatings are indispensable today, particularly for applications in internal combustion engines on piston-group (piston ring, piston pin), fuel-injection, and valve-train components (bucket tappets, finger follower) [1].

With the development of increasingly durable plastics, these materials are increasingly considered as alternatives for lightly to moderately loaded tribological components made of steel. Due to their unbeatable advantages such as their low cost, good machinability, flexibility in shaping, and low density, plastics are now increasingly considered for tribologically loaded components in bearings, gears, guide rails, etc. However, the abrasive wear of plastic surfaces under real operating conditions in the presence of dust, soot, and other wear particles emerges as a limiting factor more so than with steel.

Among the polymer types that are suitable for the mentioned applications, the PA12 (polyamide 12) und PEEK (polyetheretherketone) variants are of particular interest. Both of them possess the characteristics of high strength, good chemical resistance, high abrasion resistance, and low friction. PEEK is superior to PA12 in all respects, but is significantly more expensive to manufacture. PA12 is therefore considered a low-cost alternative to PEEK. In order to improve the mechanical properties of polymers, i.e., strength and rigidity, they are reinforced with fibers (usually glass fibers or carbon fibers). The type of fiber reinforcement depends on the specific requirements of the application, the costs, and

the desired material properties. Even if the fiber reinforcement is advantageous for the mechanical behavior in many respects, the fiber content can have a detrimental effect in the tribological respect. When in tribological contact with soft mating bodies, fibers might be more abrasive than unreinforced polymers.

The use of thin, hard, wear-protective coatings on plastic substrates analogous to steel has hardly been considered to date in industrial applications. The difference in mechanical properties between the substrate and the coating is too large and it was assumed that the coating would fail quickly due to the so-called eggshell effect. There are a few tribological studies of DLC-coated polymers in the literature, e.g., on PEEK substrates under dry conditions [2–4] or under lubricated conditions [5]. Most research has been carried out on coated polymers in the context of medical technology applications, particularly for implants [6–9]. To the best of our knowledge, there is no published work in the literature on ta-C coatings on plastic substrates apart from our own work [10].

In this study, hard and superhard ta-C-based coatings, analogous to those used as tribological protective layers on steel, were deposited on various plastics and analyzed tribologically. For this purpose, the plastics PEEK (high-quality, relatively hard plastic), PA12 (relatively inexpensive, softer plastic), and both variants with carbon-fiber reinforcement were selected as substrate materials. A standard ta-C coating and two doped variants thereof (ta-C:N and ta-C:B) served as the coating. An important issue with coatings is the use of an inter- or adhesion layer. On the one hand, the interlayer is intended to achieve a better chemical bond or mediation between the metal and the coating material, and on the other hand, it is sometimes intended to accommodate strong differences between the mechanical properties or achieve a load-supporting effect. Cr or Ti is generally used as an interlayer for metallic substrates. In this study, the Cr interlayer was also used for the plastic substrates. In a further series, ta-C:B coatings were deposited without and with two different thicknesses of the Cr interlayer for comparison.

An initial setting of tribotest parameters is used to screen three different coating variants. In a second step, the most promising coating–substrate combination with modified test conditions is then selected. Finally, a comparative tribotest is carried out with the selected variant in comparison to uncoated plastic and a coated steel reference. Even though the potential use of the coated plastics will generally take place under lubricated conditions, this first study will test the wear behavior under extreme conditions, i.e., under sliding conditions without lubrication.

## 2. Materials and Methods

For the coating and subsequent investigations, five different substrates were used (see Table 1). Four of these were different plastics from Evonik (Evonik Operations GmbH, Kirschenallee, Darmstadt, Germany), which were compared with the steel substrate AISI 52100 as a reference. The polymers included two variants each of polyamide 12 (PA12) and polyetheretherketone (PEEK). In addition to the base version, glass-fiber-reinforced PA12 and carbon-fiber-reinforced PEEK substrates were used (PA12-GF30 and PEEK-CF30, respectively). The material content of glass and carbon fibers was 30 percent. The dimensions of the sample plates were 18 mm × 13.5 mm × 3 mm. The steel surface was polished, and the surfaces of the plastics were not mechanically post-processed after injection molding.

**Table 1.** Substrate materials used for coating and their mechanical properties.

Material	AISI 52100	PA12	PA12-GF30	PEEK	PEEK-CF30
Young's Modulus [GPa]	210 *	1.4 **	6.8 **	3.5 **	24 **
Yield Strength [MPa]	>835 *	43 **	120 **	95 **	251 **

\* WIXSTEEL Industrial [11]. \*\* Evonik Industries AG product information [12].

The coatings were deposited in a commercial physical vapor deposition (PVD) chamber (VTD Vakuumtechnik Dresden GmbH, Dresden, Germany) with an attached LaserArc™



carbon evaporation source (Fraunhofer IWS, Dresden, Germany). An 8-axis planetary system was used as a sample holder and set in twofold rotation. Standard graphite targets from Plansee Composite Materials GmbH, Germany, were used as the cathode material for the generation of the ta-C and the nitrogen-gas-doped ta-C:N coatings. In the case of B-doped carbon, powder-pressed and sintered composite graphite targets with a nominal content of 5 at% of boron from the same company were used. Approximately the same content of 5 at% boron was found in the ta-C:B coating. The coating process was as follows: In the beginning, the deposition chamber was evacuated to a high vacuum at a pressure of about  $10^{-4}$  Pa and an argon ion etching process was carried out prior to the coating deposition. Subsequently, in some cases, a chromium adhesion interlayer was deposited by magnetron sputtering, followed by deposition of the carbon coatings by pulsed arc discharge that generates the carbon plasma. The arc discharges were ignited using laser pulses from a Q-switched Nd-YAG laser. Detailed information on the LaserArc process has been published elsewhere [13,14]. In the case of the ta-C:N coatings, during the evaporation of carbon by LaserArc, nitrogen gas with a 40 sccm flow rate was introduced in the deposition chamber, resulting in a content of approximately 5 at% N in the ta-C:N coating. In all process steps (ion etching, interlayer, and carbon coating) no bias voltage was used due to the use of non-conductive polymer substrates.

The coating thickness was determined using the ball crater grinding method that is standardized in EN ISO 26423:2016 [15]. Three individual craters were ground on each specimen using the calotte grinding unit "KSG 117" (Inovap GmbH, Radeberg, Germany). Instrumented indentation was carried out with a Berkovich diamond indenter on the "ZHN-1" from Zwick/Roell GmbH, Germany, to determine hardness  $H$  and the Young's modulus  $E$  of the coatings according to EN ISO 14577-4 [16]. For this purpose, the QCSM technique and the sigmoid fitting method were used for data acquisition and evaluation [17]. The maximum normal loads were 40 mN. A Poisson's ratio of 0.19 was assumed for all coatings.

For tribological characterization, an SRV4 from Optimol Instruments with the standard oscillation setup was used, which corresponds to the translatory tester according to DIN 51834-1:2010-11 [18]. The coated flat substrates were fixed as lower samples against an uncoated, polished AISI 52100 steel ball with  $\varnothing 10$  mm as the upper sample loaded with a normal load and oscillating movement. The counter-body wear was determined under the presumption of plain ball wear and was calculated via the diameter of the ball wear. The test specimen and holder were cleaned ultrasonically in high-purity benzene before the test. The tests were performed at room temperature ( $20 \pm 5$  °C) with no lubricant, in air with a controlled humidity of  $50 \pm 5\%$ .

In this study, three different parameter sets were used (see Table 2). Thereby, set I, with relatively harsh loading conditions but a short test duration, was used to obtain a quick general overview of the wear behavior on the different substrates. Set II used to simulate a load case that is closer to the application. The normal force is reduced to a tenth of the previous load and the test duration is extended by a factor of 10. Set III was only applied to selected substrates and is intended to show the limits in terms of load and load-bearing capacity.

**Table 2.** Parameter sets used for tribological characterization.

Parameter	Set I	Set II	Set III
Normal load [N]	10	1	10
Oscillation frequency [Hz]	10	10	10
Stroke [mm]	1	1	1
Testing time [min]	10	100	60

The white-light interferometry method was used to determine the surface roughness  $S_a$  using the Leica DCM 3D microscope according to EN ISO 25178 [19].

Particles and defects visible on the surface, i.e., carbon macroparticles incorporated in the coating, were quantified by the “surface defect fraction (SDF)” parameter that was determined using three individual light microscopy images from different positions at the surface at 500 $\times$  magnification. More information about the method to determine the SDF parameter can be found elsewhere [20].

### 3. Results

First, a coating series of ta-C, ta-C:N, and ta-C:B with nominal 1  $\mu\text{m}$  thicknesses were deposited on all substrates, using a Cr interlayer with about a 0.1  $\mu\text{m}$  thickness. The compilation in Figure 1 shows the surface topography of the different substrates in the initial state and with a 1  $\mu\text{m}$  ta-C coating. The PA12 and PEEK substrates are initially very smooth. The coating creates a crack pattern on the soft PA12. This has no negative effect on adhesion. With PEEK, on the other hand, the surface remains smooth. However, existing scratches are intensified by the coating, which can be seen in the interference contrast. The fiber-reinforced substrates are initially rougher, whereby the glass fibers in the soft PA12 matrix are not clearly visible. However, the fibers are significantly more pronounced due to the coating and the deformation of the surface. In the case of fiber-reinforced PEEK, the fibers are clearly visible on the surface. After coating the fibers are covered and their visibility is reduced.

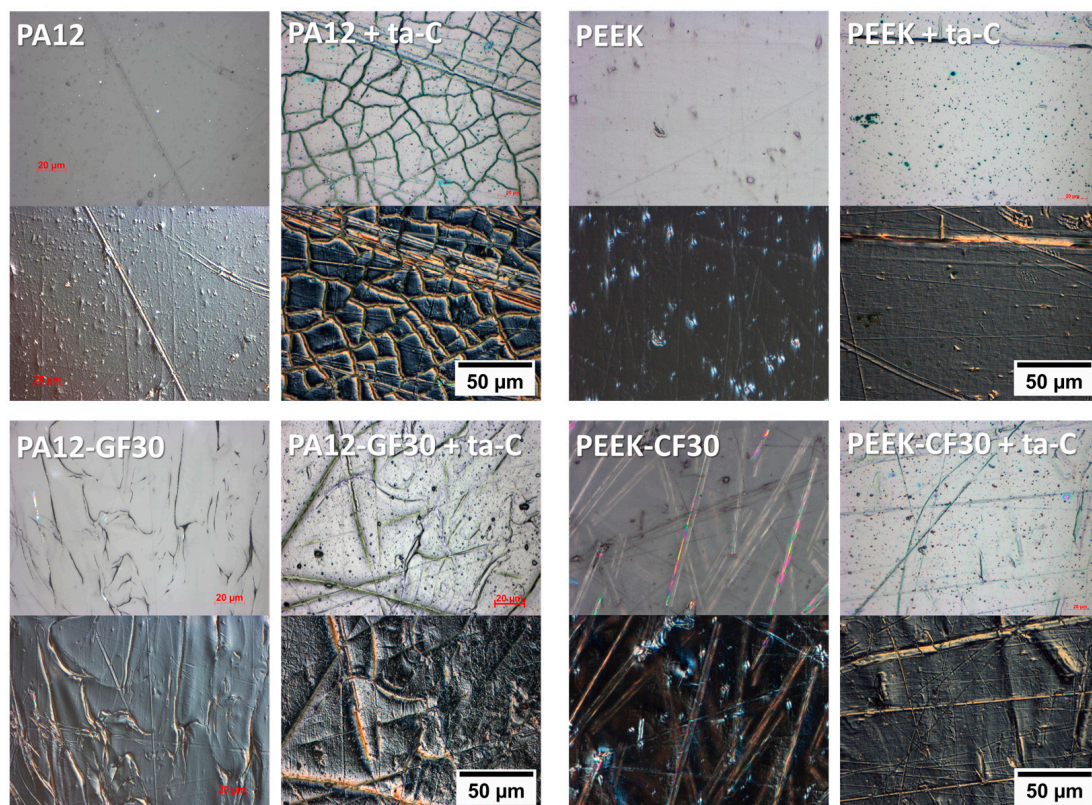


**Figure 1.** Microscopic images of the PA12, PA12-GF30, PEEK, and PEEK-CF30 uncoated (left), and 1  $\mu\text{m}$  ta-C-coated (right) substrates in bright field (top) and with differential interference contrast (DIC) filter (bottom).

A decisive parameter is the surface defect fraction (SDF), which provides information on the extent to which the surface is covered with coating defects. These defects are unavoidable in arc coating processes and result in unfavorable roughness on the surface, which is associated with high wear in tribological contacts, especially on the counter body. The SDF parameter is more sensitive for detecting the effects of coating defects on the

tribological behavior than surface roughness parameters. However, it is very instructive to compare the effect of the coating on both parameters.

As for the roughness parameter  $S_a$ , the steel surface showed very little change due to the coatings (Figure 2 (top)). PA12, on the other hand, was initially rather smooth, but showed a strong increase in  $S_a$  due to the coatings. The same applies to PA12-GF30, even if its initial roughness was significantly greater than that of PA12. In contrast, the two PEEK variants—similar to steel—did not show such strong changes in roughness as the PA12 variants. Here, the low roughness with the coating was retained, which was also the case for the fiber-reinforced PEEK.

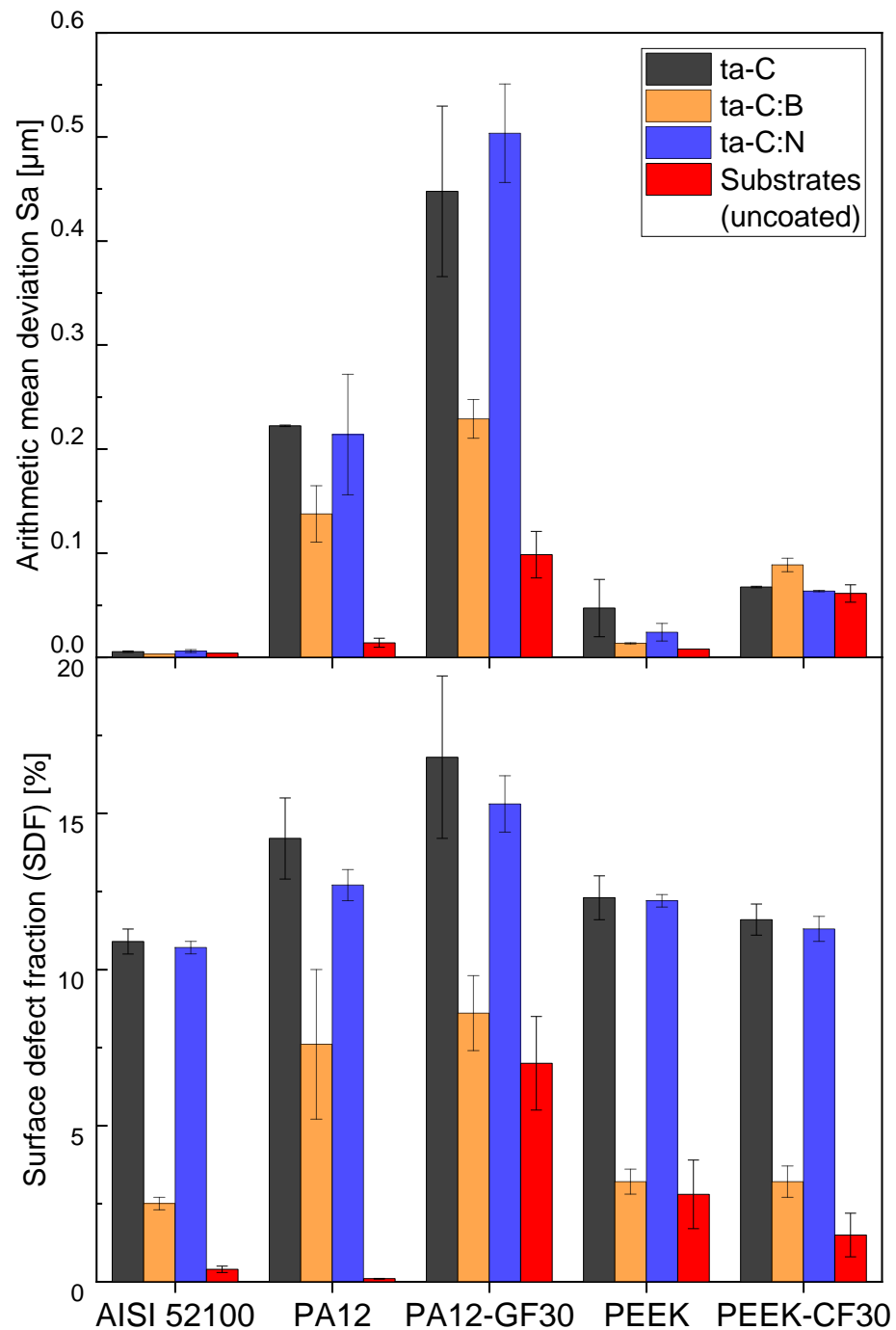


**Figure 2.** Arithmetic mean deviation  $S_a$  (top) and surface defect fraction (SDF) (bottom) for AISI 52100, PA12, PA12-GF30, PEEK, and PEEK-CF30 uncoated and coated with 1  $\mu\text{m}$  ta-C, 1  $\mu\text{m}$  ta-C:N, and 1  $\mu\text{m}$  ta-C:B.

The SDF values (Figure 2 (bottom)) showed strong variations for the different coatings, but the nature of the changes depending on the coating type was the same for all substrate variants. This shows that the SDF parameter reacts very sensitively to coating-specific surface defects, with the ta-C:B film having the lowest SDF in all coated cases. The SDFs of ta-C and ta-C:N were very similar because the coating plasma is identical except for the N<sub>2</sub> gas inlet. In the case of ta-C:B, there were far fewer defects. This is already known from previous work [11], and therefore, this coating was favored over the other coating types.

The results of the basic characterization of these coatings are summarized in Table 3. Due to the large difference in properties between the coatings and the plastic substrates, it was not possible to determine any mechanical properties. Therefore, all values were determined on the coatings deposited on AISI 52100 steel substrates.

**Table 3.** Measured coating properties \*.

Coating	Thickness [μm]	Hardness [GPa]	E-Modulus [GPa]	SDF [%]
ta-C	1.2 ± 0.1	37.2 ± 0.6	408 ± 12	10.9 ± 0.4
ta-C:N	1.4 ± 0.1	26.8 ± 1.3	303 ± 23	10.7 ± 0.2
ta-C:B	0.9 ± 0.2	48.1 ± 1.7	567 ± 14	2.5 ± 0.2

\* Coatings deposited on polished AISI 52100 steel substrates.

It should be noted that the hardness of the ta-C coating was rather moderate compared to the common literature data for ta-C. This is due to the fact that no bias voltage was used in the processes to accelerate the ions in the coating plasma, as is typically done. In our case, the intrinsic kinetic ion energy of the carbon species in the plasma is crucial for the formation of sp<sup>3</sup> bonds, and hence, the hardness of ta-C. Consequently, the hardness decreases in the case of ta-C:N because the energy of some coating particles was slowed down by collisions with N<sub>2</sub> molecules due to the gas inlet. In the case of ta-C:B, on the other hand, the hardness increased compared to ta-C. This is presumably due to the fact that during the evaporation of B-doped graphite in the arc process, higher particle energies were present than in a pure carbon plasma. This is the subject of current investigations on plasma particle energy distribution.

### 3.1. Wear Behavior of Different Coating Types

Using parameter set I in tribotesting (see Table 2), the wear behavior of coatings on different substrates and the wear of uncoated steel-ball counter bodies were analyzed. In these tests, the three coating types, ta-C, ta-C:N, and ta-C:B including the 0.1 μm Cr interlayer (see Table 3), were investigated. The wear images are summarized in Table 4.

A volumetric determination of the wear abrasion from the coatings is not possible with the plastic samples due to the significant deformation. Therefore, only a qualitative assessment can be made here. However, it was possible to determine the counter-body wear on the steel balls and the result is summarized in Figure 3.

**Table 4.** Optical images of wear tracks on the coatings and counter body (steel ball) on different coatings after tribotests with set I.

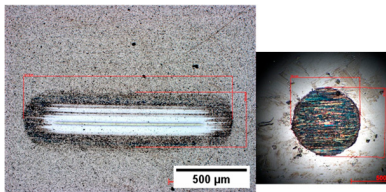
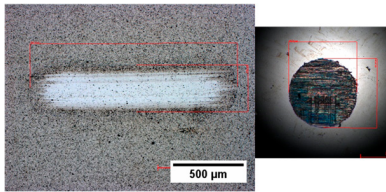
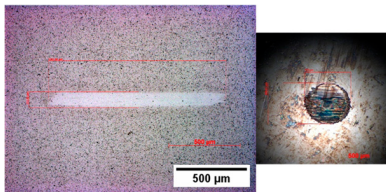
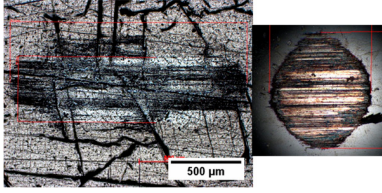
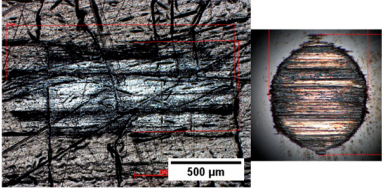
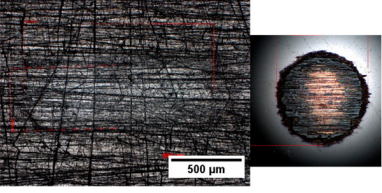
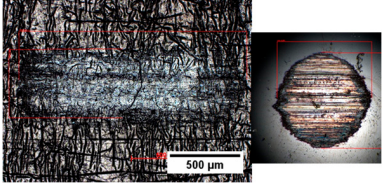
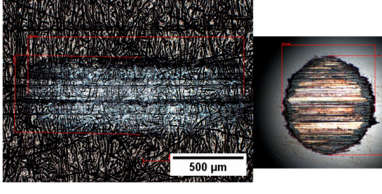
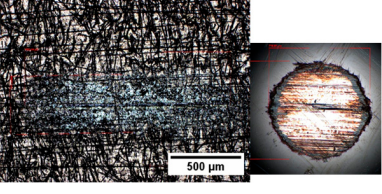
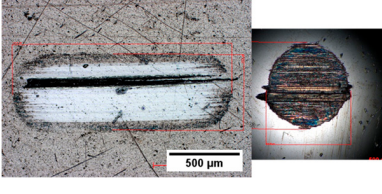
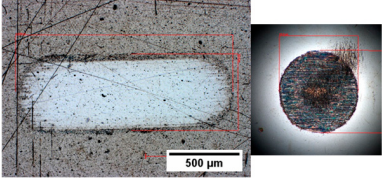
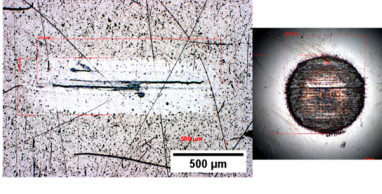
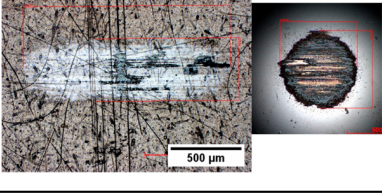
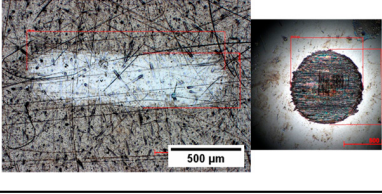
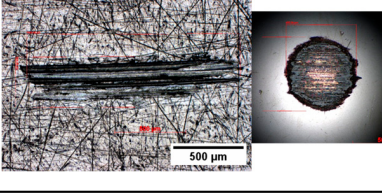
Substrate	Coating		
	ta-C	ta-C:N	ta-C:B
AISI 52100			



Table 4. Cont.

Substrate	Coating		
	ta-C	ta-C:N	ta-C:B
PA12			
PA12-GF30			
PEEK			
PEEK-CF30			

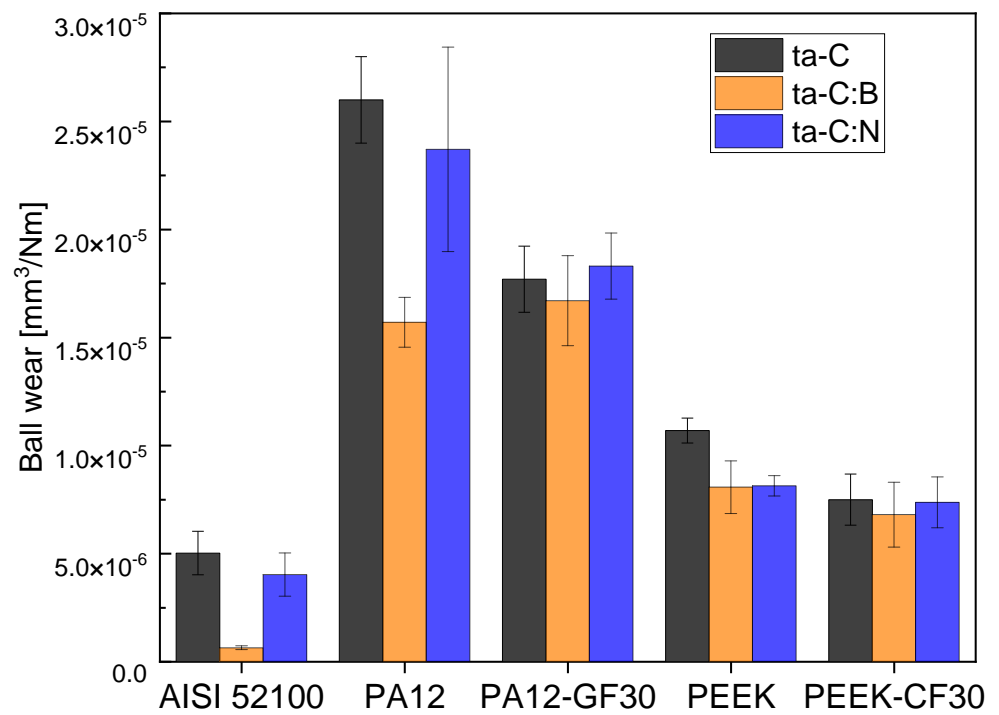


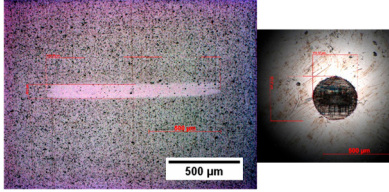
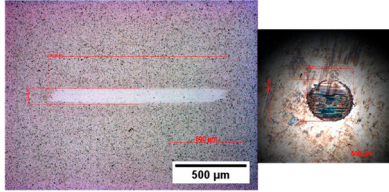
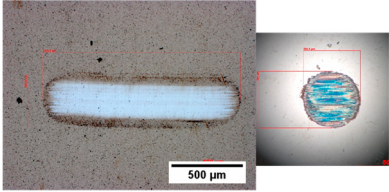
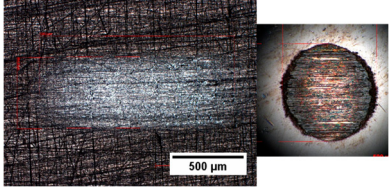
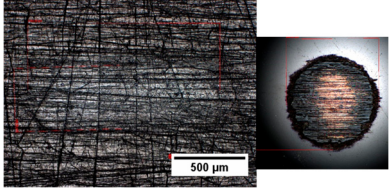
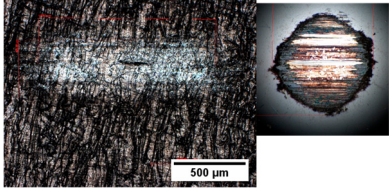
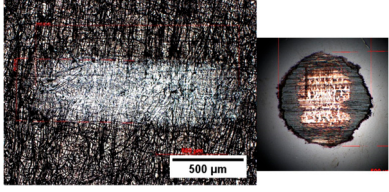
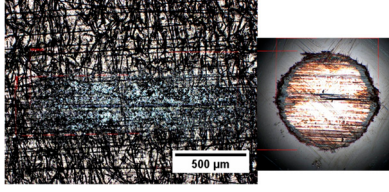
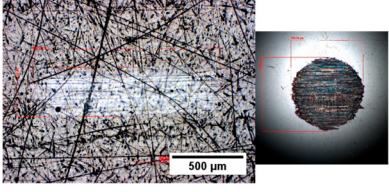
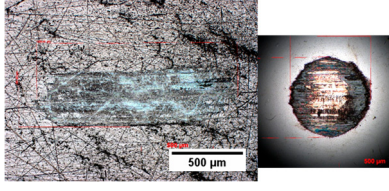
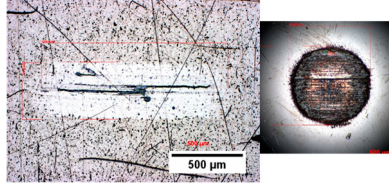
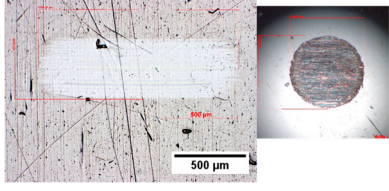
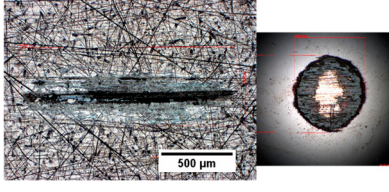
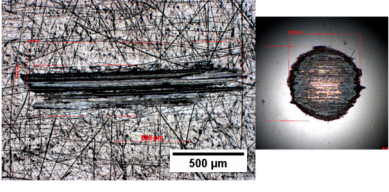
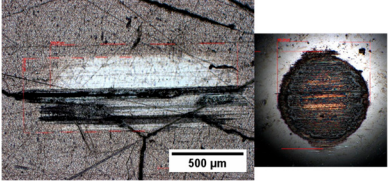
Figure 3. Steel-ball counter-body wear measured after tribotests with set I.



### 3.2. Influence of the Cr Interlayer on Wear Behavior

The investigations into the influence of the Cr interlayer were carried out with the ta-C:B (1  $\mu\text{m}$ ) coating variant. A variant without a Cr layer, a variant with 0.1  $\mu\text{m}$  Cr, and a variant with 0.5  $\mu\text{m}$  Cr were produced and tested in the tribometer. The tribotest parameters were the same as before (set I) and wear images are summarized in Table 5.

**Table 5.** Optical images of wear tracks on the coatings and counter body (steel ball) on ta-C:B-coatings with different interlayers after tribotests with set I.

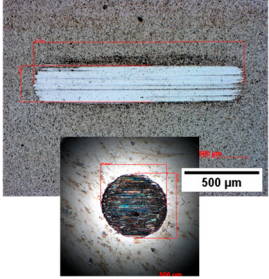
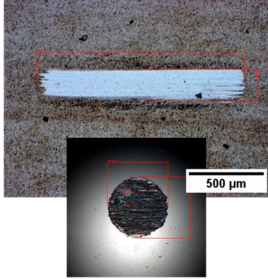
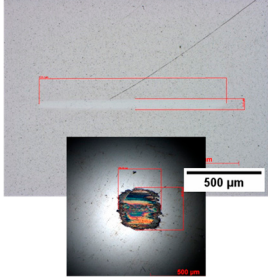
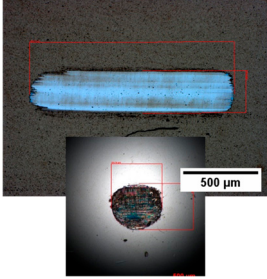
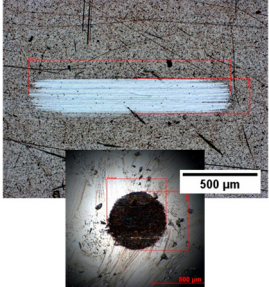
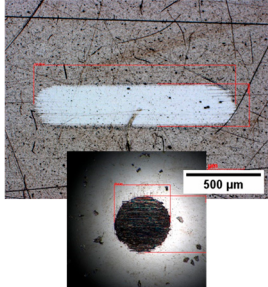
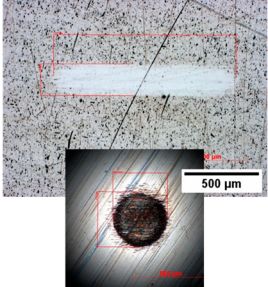
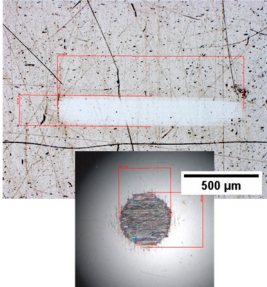
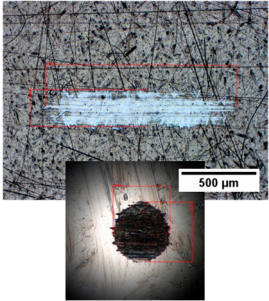
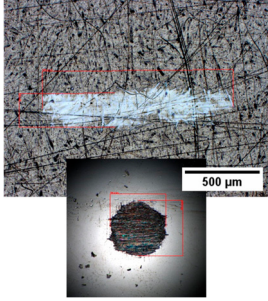
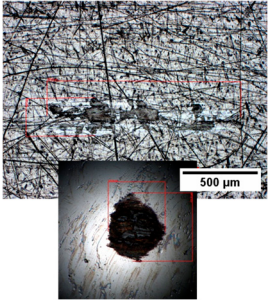
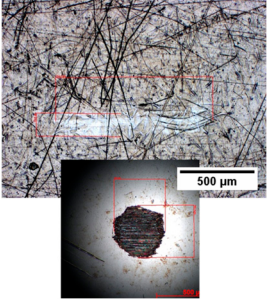
Substrate	Coating		
	ta-C:B	0.1 $\mu\text{m}$ Cr + ta-C:B	0.5 $\mu\text{m}$ Cr + ta-C:B
AISI 52100			
PA12			
PA12-GF30			
PEEK			
PEEK-CF30			

### 3.3. Wear Behavior under Long-Time Testing Conditions

In this series, using tribotest parameter set II, a reduced normal load but extended testing time of 100 min was used (see Table 2). The aim of this series of tests was to make a comparison between the coating variants under comparatively mild but application-related load conditions. Due to the fact that, in previous investigations, the mating body wear on the PA12 and PA12-GF30 substrates was rather high, these tests were limited to the PEEK and PEEK-CF30 substrates (Table 6).



**Table 6.** Optical images of wear tracks on coatings and counter body (steel ball) on selected coating–substrate systems after tribotesting with parameter set II.

Substrate	Coating			
	0.1 $\mu\text{m}$ Cr + ta-C	0.1 $\mu\text{m}$ Cr + ta-C:N	0.1 $\mu\text{m}$ Cr + ta-C:B	0.5 $\mu\text{m}$ Cr + ta-C:B
AISI 52100				
PEEK				
PEEK-CF30				

### 3.4. Comparison of the Load-Bearing Capacity

In this final tribotest, a comparison was made between a selected coated plastic variant with an analogously coated steel substrate and uncoated plastic. The high standard load of 10 N was again applied with the new parameter of set III, which, in contrast to set I, consisted of a test duration of 60 min. In these tests, the characteristics of the friction coefficients over the test duration were also examined.

The coating variant 0.1  $\mu\text{m}$  Cr + 1  $\mu\text{m}$  ta-C:N was selected as a suitable coating for this test. Although this did not have the lowest counter-body wear (like ta-C:B), it proved to be the most robust variant overall in the previous tests. The fact that no grooves or scratches were observed in the coating of ta-C:N after the wear tests was also considered favorable.

It can be seen that the ta-C:N-coated substrates were at a much lower friction level than the uncoated PEEK. This also shows damage that goes beyond abrasive wear removal. The surface appeared heavily deformed in the area of the wear track. Even if the coating wear was lowest on the steel substrate, the wear track of the ta-C:N on the PEEK substrate appeared basically similar in appearance. The coating generally withstood the load, but there were already coating breakthroughs in some areas. On one sample (see dashed arrow in Figure 4), the coating penetration also manifested itself in a sudden increase in the coefficient of friction.

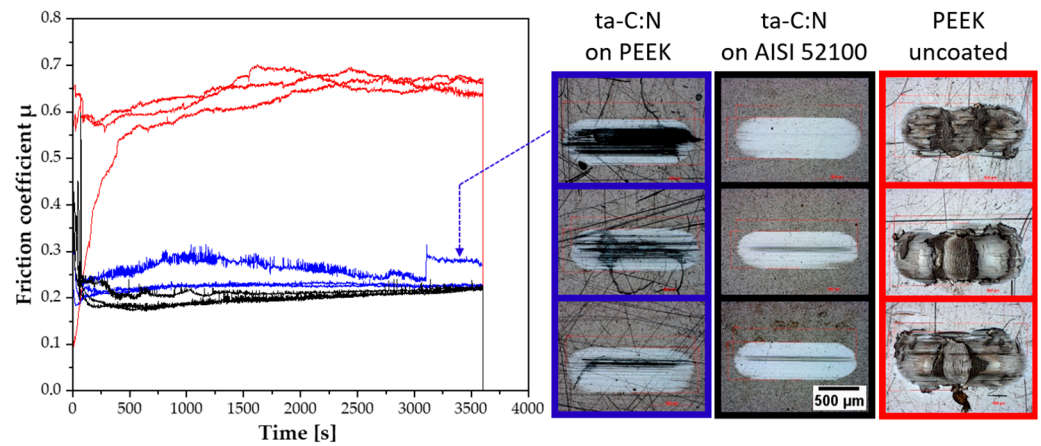


**Figure 4.** Comparison of friction coefficients (left) and coating/surface wear behavior between ta-C:N-coated steel (black) and PEEK (blue) vs. an uncoated PEEK (red) sample (right).

#### 4. Discussion

In order to interpret the results of the tribological measurements, it is first necessary to consider the different mechanical contact situations of the various material pairings. The large differences in the modulus of elasticity between AISI 52100 steel and the plastics lead to very different Hertzian contact conditions. For example, the plastics have a much larger contact area, but smaller contact stress at the same load compared to steel. In order to analyze the stress distribution in terms of Hertz's contact theory, the stresses for all materials including a 1  $\mu\text{m}$  thick ta-C topcoat were calculated using FilmDoctor software (SIO<sup>®</sup> Saxonian Institute of Surface Mechanics, Ummanz, Germany, <https://siomec.com/software/filmdoctor-studio/>, accessed on 12 September 2024) for the two normal loads of 10 N (parameter sets I and III) and 1 N (set II). The calculations were based on the assumption of purely elastic behavior of all materials. The parameters used for the calculations were the characteristic values of the materials from Tables 1 and 3. The results are shown as examples for steel, PEEK, and PEEK-CF30 in Figure 5.

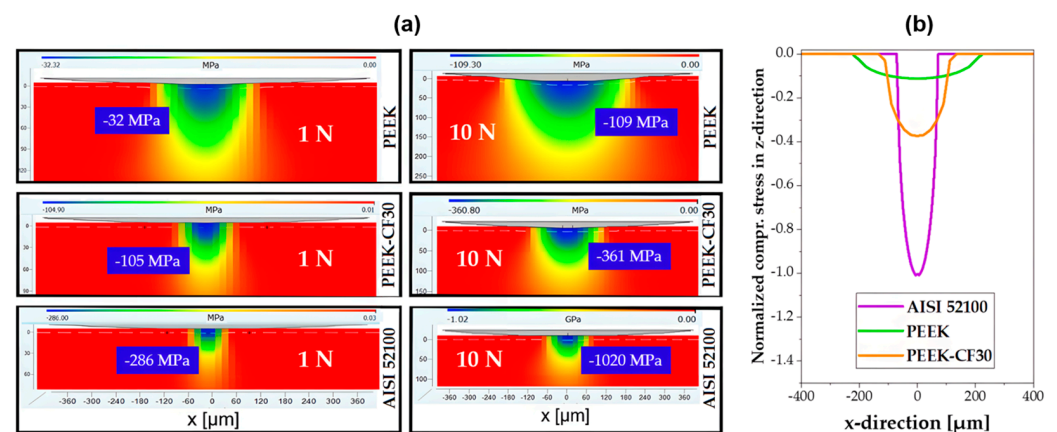


**Figure 5.** Visualization of the calculated stress distribution of the normal stress  $\sigma_z$  for three different substrate materials with 1  $\mu\text{m}$  ta-C coating vs. steel ball with 1 N and 10 N normal load (a) and distribution of  $\sigma_z$  at  $z = 0$  in  $x$ -directions at 10 N normal load (b).

As expected, the results show large differences in the contact surfaces, the level of compressive stress generated in the substrate by the ball indentation, and the different spatial distributions of the stress in the substrate. In this way, it becomes clear why the track widths of the coatings on the plastics in the wear tests are always wider than on the coated AISI 52100 steel ( $\approx 500 \mu\text{m}$  vs.  $\approx 150 \mu\text{m}$ ). It is now also clear why the counter-body wear

values (ball abrasion) with the same coatings were significantly higher with the plastics than with steel (see Tables 4 and 5). With the softer substrates, the balls come into contact with a larger area of the abrasive coating surface. It is important to take a closer look at the special features of ta-C-based coatings deposited using arc technology: coatings deposited using a vacuum arc-evaporation process always exhibit unavoidable growth defects due to droplets or macroparticles, which are incorporated into the coating during deposition and increasingly cause roughness peaks on the ta-C-based coatings as the coating thickness increases. The SDF parameter (see Section 3) describes the phenomenon quantitatively. The higher the SDF value, the more abrasive the coating. Two things need to be mentioned in this context: (I) Due to the coating defects, the counter-body wear is initially very high. However, this is primarily a running-in effect. (II) The roughness peaks do not only wear the counter body. By breaking out some defects, a micro-abrasive material is generated, and the coating also suffers wear. The ta-C:B coating is distinguished from the other two coating types by a much lower SDF-value (see Table 3). This phenomenon, described in [14], makes this coating variant more advantageous compared to the other two variants, ta-C and ta-C:N, with high SDF values.

When looking at the results from Section 3.1, the comparison of the coating variants in an initial tribo-screening test, the previously discussed points are particularly important for the interpretation of the results. The counter-body wear is significantly less pronounced with ta-C:B than with the other two coatings. This is particularly evident with the steel variant, but also with PA12. Another noticeable aspect in Figure 4 is that the counter-body wear is much higher for the plastics and especially for the two PA12 variants than for steel. This is explained by the differences in the contact areas discussed above: the softer the substrate, the larger the contact area and the greater the amount of wear particles the steel ball is exposed to in the friction contact. Additionally, regarding the results in Section 3.1, it should be noted that despite the comparatively high load, complete coating failure occurred in only one case (ta-C on PA12). In most other cases of coated plastic substrates, the coatings exhibited grooves, scratches, and cracks in addition to abrasive wear, but remained largely intact. The ta-C:N coatings left the best impression, especially on PEEK and PEEK-CF30. After the tribotest, these coatings were still largely intact and showed a relatively smooth surface in the wear track. The behavior of the ta-C:N coating on the PEEK substrates was still worse than on steel, but it came closest to steel in the appearance of the wear behavior.

To test the influence of the adhesion layer on the tribological performance, the ta-C:B variant was selected due to its lowest coating roughness. The results presented in Section 3.2 show a differentiated picture. Basically, it can be initially said that with all adhesion layer variants, including without a Cr adhesion layer, there appears to be good adhesion strength of the coatings with one exception, the 0.5  $\mu\text{m}$  thick Cr layer on the PEEK-CF30 substrate. In terms of wear behavior, both for the counter body and the coating, the thick adhesion layer (0.5  $\mu\text{m}$ ) shows a tendency to improve the tribological performance of the coated plastics. This is attributed to an improved load-supporting effect of the now approximately 1.5  $\mu\text{m}$  thick coating system compared to the other coatings ( $\approx 1$   $\mu\text{m}$  coating thickness). However, the advantages are not too significant and, as mentioned, in one case, there was also a failure with the 0.5  $\mu\text{m}$  thick Cr adhesion layer.

The focus of the tribotests in the next step was to subject promising coating–substrate combinations to significantly longer test durations under more application-oriented conditions (lower load) with parameter set II (see Table 2). The results in Table 6 with the two PEEK and four coating variants compared to the analogously coated steel show a very good performance of the coatings. Overall, the wear of the counter body and the wear tracks in the coatings were now more similar to the coated steel samples than in the previous tests with the tribo-parameter set I. This is because, in these tests, the running-in process was obviously completed and a more stable tribological situation had established itself, which did not depend as much on the roughness and defects of the coating surface.

In the final tribotest, the overall most-promising plastic-coating system was compared to an uncoated plastic and an analogously coated steel substrate under demanding testing



conditions. The PEEK substrate selected for this, with a 1  $\mu\text{m}$  thick ta-C coating, showed similarly low friction values to the coated steel (see Section 3.4). However, it can be seen that the system has reached the limits of its load capacity after the 60 min test. Initial coating perforations indicated that the coating was about to fail, as can be seen in Figure 4. The uncoated PEEK suffered serious damage in the tribotest. Presumably, incipient plastic deformation coupled with abrasive wear could already be observed here.

Overall, it can be stated that the ta-C:N coating greatly improved the load-bearing capacity of the PEEK. The tribological behavior of the system is very similar to that of the ta-C:N-coated steel substrate, even if—as mentioned above—the service life is limited under these harsh conditions.

## 5. Conclusions

In this article, it is shown that, contrary to expectations, superhard ta-C-based coatings can be used as a tribological protective layer on soft-plastic substrates, even under unlubricated conditions. The adhesion of all the coating variants examined on the four plastic substrates was generally good, with no “eggshell effect” observed.

The ta-C, ta-C:N, and ta-C:B coatings showed similar tribological behavior, caused by the relatively high coating roughness. In all cases, a pronounced running-in behavior with high counter-body wear was observed. The ta-C:B coatings, with their naturally lower defect density, were advantageous in terms of counter-body wear. The studies also revealed that an adhesion-promoting interlayer of Cr is helpful in some cases (better load-supporting effect), although the coatings also work on plastic substrates without a Cr adhesion layer.

Overall, the study concludes that the performance of plastic substrates can be significantly improved by hard or superhard coatings of ta-C, ta-C:N, and ta-C:B, even under harsh tribological conditions, at least for relatively short testing times. Despite the extreme hardness difference and the roughness of the coatings, the systems show promising tribological behaviors in air, coming quite close to that of an analogously coated steel substrate.

In future, there are several possibilities to improve the coating performance due to reducing the defect density (through plasma filtering) and running-in layer concepts, i.e., graded soft top layers that are supposed to mitigate counter-body wear and thus improve the running-in behavior.

**Author Contributions:** Conceptualization, F.K. and V.W.; investigation, P.N.; writing—original draft preparation, V.W.; writing—review and editing, F.K.; supervision and project administration, F.K.; funding acquisition, V.W. All authors have read and agreed to the published version of the manuscript.

**Funding:** This research was funded by BMWK (Federal Ministry for Economic Affairs and Climate Action, Germany) within the project Chephren (03EN4005E), and by the Fraunhofer Internal Program SupraSlide under Grant No. PREPARE 840066.

**Data Availability Statement:** Data available on request due to restrictions.

**Acknowledgments:** The authors would like to thank Evonik Operations GmbH (Kirschenallee, Darmstadt, Germany) for providing the plastic substrates used in this research. We also acknowledge Stefan Makowski, Fabian Härtwig, and Paul Skorloff from the Fraunhofer IWS for their support during the experimental work.

**Conflicts of Interest:** The authors declare no conflicts of interest.

## References

1. Kano, M. *Overview of DLC-Coated Engine Components*; Cha, S., Erdemir, A., Eds.; Coating Technology for Vehicle Applications; Springer International Publishing: Berlin/Heidelberg, Germany, 2015.
2. Kaczorowski, W.; Szymanski, W.; Batory, D.U.; Niedzielski, P. Tribological properties and characterization of diamond like carbon coatings deposited by MW/RF and RF plasma-enhanced CVD method on poly(ether-ether-ketone). *Plasma Process Polym.* **2014**, *11*, 878–887. [[CrossRef](#)]
3. Watanabe, Y.; Suzuki, H.; Nakamura, M. Improvement of the tribological property by DLC coating for environmentally sound high polymer materials. *Int. J. Mater. Prod. Technol.* **2001**, *2*, 787–792.



4. Tomaszewski, P.K.; Pei, Y.T.; Verkerke, G.J.; De Hosson, J. Improved tribological performance of PEEK polymers by application of diamond-like carbon coatings. *Eur. Cells Mater.* **2024**, *27*, 4.
5. Reitschuster, S.; Maier, E.; Lohner, T.; Stahl, K.; Bobzin, K.; Kalscheuer, K.; Thiex, M.; Sperka, P.; Hartl, M. DLC-Coated Thermoplastics: Tribological Analyses under Lubricated Rolling-Sliding Conditions. *Tribol. Lett.* **2022**, *70*, 121. [[CrossRef](#)]
6. Rothhammer, B.; Marian, M.; Neusser, K.; Bartz, M.; Böhm, T.; Krauß, S.; Schroeder, S.; Uhler, M.; Thiele, S.; Merle, B.; et al. Amorphous carbon coatings for total knee replacements—Part II: Tribological behavior. *Polymers* **2021**, *13*, 1880. [[CrossRef](#)] [[PubMed](#)]
7. Puertolas, J.A.; Martinez-Nogues, V.; Martinez-Morlanes, M.J.; Mariscal, M.D.; Medel, F.J.; Lopez-Santos, C.U.; Yubero, F. Improved wear performance of ultra high molecular weight polyethylene coated with hydrogenated diamond like carbon. *Wear* **2010**, *269*, 458–465. [[CrossRef](#)]
8. Onate, J.I.; Comin, M.; Bracerias, I.; Garcia, A.; Viviente, J.L.; Brizuela, M.; Garagorri, N.; Peris, J.L.U.; Alava, J.I. Wear reduction effect on ultra-high-molecular-weight polyethylene by application of hard coatings and ion implantation on cobalt chromium alloy, as measured in a knee wear simulation machine. *Surface Coat. Technol.* **2001**, *142–144*, 1056–1062. [[CrossRef](#)]
9. Wang, H.; Xu, M.; Zhang, W.; Kwok, D.T.K.; Jiang, J.; Wu, Z.; Chu, P.K. Mechanical and biological characteristics of diamond-like carbon coated poly aryl-ether-ether-ketone. *Biomaterials* **2010**, *31*, 8181–8187. [[CrossRef](#)] [[PubMed](#)]
10. Rothhammer, B.; Schwendner, M.; Bartz, M.; Wartzack, S.; Böhm, T.; Krauß, S.; Merle, B.; Schroeder, S.; Uhler, M.; Kretzer, J.P.; et al. Wear Mechanism of Superhard Tetrahedral Amorphous Carbon (ta-C) Coatings for Biomedical Applications. *Adv. Mater. Interfaces* **2023**, *10*, 2202370. [[CrossRef](#)]
11. WIX WIXSTEEL Industrial, Product Information. Available online: <https://www.wixsteel.com/products/alloy-steel-bar/ball-bearing-steel-bar/100cr6> (accessed on 12 September 2024).
12. EVO Evonik Industries AG, Product Information. Available online: <https://www.plastics-database.com> (accessed on 12 September 2024).
13. Kaulfuss, F.; Weihnacht, V.; Zawischa, M.; Lorenz, L.; Makowski, S.; Hofmann, F.; Leson, A. Effect of Energy and Temperature on Tetrahedral Amorphous Carbon Coatings Deposited by Filtered Laser-Arc. *Materials* **2021**, *14*, 2176. [[CrossRef](#)] [[PubMed](#)]
14. Krülle, T.; Kaulfuß, F.; Weihnacht, V.; Hofmann, F.; Kirsten, F. Amorphous Carbon Coatings with Different Metal and Nonmetal Dopants: Influence of Cathode Modification on Laser-Arc Evaporation and Film Deposition. *Coatings* **2022**, *12*, 188. [[CrossRef](#)]
15. *DIN EN ISO 26423:2016-11*; Fine Ceramics (Advanced Ceramics, Advanced Technical Ceramics)—Determination of Coating Thickness by Crater-Grinding Method. International Organization for Standardization: Geneva, Switzerland, 2016.
16. *DIN EN ISO 14577-4:2017-04*; Metallic Materials—Instrumented Indentation Test for Hardness and Materials Parameters—Part 4: Test Method for Metallic and Non-Metallic Coatings. International Organization for Standardization: Geneva, Switzerland, 2017.
17. Lorenz, L.; Chudoba, T.; Makowski, S.; Zawischa, M.; Schaller, F.; Weihnacht, V. Indentation modulus extrapolation and thickness estimation of ta-C coatings from nanoindentation. *J. Mater. Sci.* **2021**, *19*, 3. [[CrossRef](#)]
18. *DIN 51834-1:2010-11*; Testing of Lubricants—Tribological Test in the Translatory Oscillation Apparatus—Part 1: General Working Principles. German Institute for Standardization: Berlin, Germany, 2010.
19. *DIN EN ISO 25178-2:2023-09*; Geometrical Product Specifications (GPS)—Surface Texture: Areal—Part 2: Terms, Definitions and Surface Texture Parameters. International Organization for Standardization: Geneva, Switzerland, 2023.
20. Krülle, T.; Peritsch, P.; Kaulfuß, F.; Bui Thi, Y.; Zawischa, M.; Weihnacht, V. Investigation of surface defects on doped and undoped carbon coatings deposited by Laser Arc Technology using an optical surface quantification method. *Jahrb. Oberflächentechnik* **2021**, *77*, 233–247.

**Disclaimer/Publisher’s Note:** The statements, opinions and data contained in all publications are solely those of the individual author(s) and contributor(s) and not of MDPI and/or the editor(s). MDPI and/or the editor(s) disclaim responsibility for any injury to people or property resulting from any ideas, methods, instructions or products referred to in the content.